Nonequilibrium distributions from the Fokker-Planck equation: Kappa distributions and Tsallis entropy

Alp Doga Oylukan
Department of Mathematics University of British Columbia Vancouver, British Columbia V6T 1Z4, Canada

Bernard Shizgal
Institute of Applied Mathematics University of British Columbia Vancouver, British Columbia V6T 1Z4, Canada

(Received 18 January 2023; accepted 15 June 2023; published 7 July 2023)

Nonequilibrium systems in chemistry and physics are generally modeled with the Boltzmann, Fokker-Planck, and Master equations. There has been a considerable interest in the nonequilibrium distributions of electrons and ions in space physics in different environments as well as in other systems. An often-used empirical model to characterize these distributions, especially in space physics, is the Kappa distribution. There have been numerous efforts to provide a theoretical basis for the Kappa distribution that include the Fokker-Planck equation with specific drift and diffusion coefficients. Alternatively, the maximization of the Tsallis nonextensive entropy provides the desired Kappa distribution. This paper examines three families of Fokker-Planck equations that provide a steady-state Kappa distribution as well as a myriad of other nonequilibrium distributions. The relationship of these works with analogous studies of distributions with asymptotic high-energy tails is also considered. It is clear that the many different nonequilibrium distribution functions that can occur cannot all be rationalized with Gibbs-Boltzmann statistical mechanics, which uniquely gives equilibrium distributions, or with the Tsallis nonextensive entropy, which gives uniquely the Kappa distribution. The current research is directed towards an improved understanding of the origin of nonequilibrium distributions in several specific systems.

DOI: 10.1103/PhysRevE.108.014111

I. INTRODUCTION

The study of nonequilibrium systems in chemistry and physics has been a very active research area for decades. There has been considerable research effort directed towards the determination of particle distribution functions in chemical reactions [1–3], vibrational nonequilibrium [4–7], neutron transport [8,9], space physics [10–15], lasers, and other diverse systems such as laser cooling and trapping [16]. The historical approach to nonequilibrium effects is the determination of transport coefficients in dilute gases based on the Boltzmann equation [17] or in terms of irreversible thermodynamics [18] analogous to recent discussions of stochastic thermodynamics [19–21]. The transport properties of neutrons in. nuclear reactors is treated in a similar fashion [8,9]. The study of the mobilities of ions dilutely dispersed in a heat bath of neutrals under the influence of an external electric field is based on the Boltzmann equation [22]. In his book, Viehland provides an excellent historical accounting of the development of theoretical methods to study and explain the origin of nonequilibrium phenomena. A similar discourse was provided by Robson *et al.* [23] on charged particle transport in gases and condensed matter. The statistical mechanics of classical liquids is presented by Santos [24] with historical discussions.

In the study of these nonequilibrium physical situations, the theoretical approach is to determine the distribution functions from the appropriate transport equation. It is useful to note the derivation of the Fokker-Planck equation (FPE) [25] from the hard-sphere Boltzmann equation [26] for the time evolution of the distribution function for heavy test particles (M) dilutely dispersed in a large excess of light particles (m). The "Rayleigh" FPE for this system is

$$\frac{\partial P(y,t)}{\partial t} = -k_R \frac{\partial}{\partial y}\left\{(y-3/2)P(y,t) + \frac{\partial}{\partial y}[yP(y,t)]\right\},\quad y \in [0,\infty), \tag{1}$$

where $y = Mv^2/2k_BT_b$ is the reduced energy $k_R = \frac{16}{3}\frac{M}{m}N_2\pi(d_{12}^2/4)\sqrt{2k_BT_b/\pi m}$, where T_b is the bath temperature, πd_{12}^2 is the hard-sphere cross section, and k_B is the Boltzmann constant. It is clear from Eq. (1) that an arbitrary initial distribution will relax to a Maxwellian, $P_{\max}(y) = (2/\sqrt{\pi})\sqrt{y}e^{-y}$. For the time evolution of the distribution function of light particles (of mass m) dilutely dispersed in a heat bath of heavy particles (of mass M), we have the "Lorentz" FPE [26],

$$\frac{\partial P(x,t)}{\partial t} = -k_L \frac{\partial}{\partial x}\left\{(3-2x^2)P(x,t) + \frac{\partial}{\partial x}[xP(x,t)]\right\},\quad x \in [0,\infty), \tag{2}$$

where $x = \sqrt{mv^2/2k_BT_b}$ is the reduced speed and $k_L = 2\frac{m}{M}N_2\pi d_{12}^2\sqrt{2k_BT_b/\pi m}$. It is clear from Eq. (2) that an arbitrary initial nonequilibrium distribution will relax to the equilibrium Maxwellian distribution, $P_{\max} = (4/\sqrt{\pi})x^2e^{-x^2}$. The relaxation to Maxwellian distributions is a dynamical result owing to the structure of the respective Fokker-Planck equations. The analogous approach of the population of vibrational states of a diatomic molecule is described with an analogous Master equation [27,28].

The Lorentz-FPE has been applied to numerous realistic electron-atom systems [29–31]. These systems are not equilibrium systems so that classical thermodynamics and entropy principles do not play a role. For nonequilibrium systems, the appropriate formalism is irreversible thermodynamics [18,32]. The current paper considers the physics involved in the creation of steady nonequilibrium distributions which are non-Boltzmann distributions, in particular Kappa distributions, that feature prominently in space physics [11,15] as discussed in the following paragraphs.

There have been numerous studies in space physics that show that nonequilibrium particle distributions are often well fitted with the Kappa distribution [11,15,33–36] defined by

$$f_\kappa(x) = C(\kappa)\left[\frac{1}{1+\frac{x^2}{\kappa+1}}\right]^{\kappa+1}, \tag{3}$$

where the dimensionless speed is $x = v/v_{\text{th}}$, where $v_{\text{th}} = \sqrt{2k_BT_b/m}$ is the thermal speed, m is the particle mass, and T_b is the bath temperature. The κ dependence in Eq. (3) is the form derived in Ref. [11] which differs slightly from other forms [15]. The three dimensional Kappa distribution is normalized according to $4\pi\int_0^\infty f_k(x)x^2dx = 1$ so that $C(\kappa) = \Gamma(\kappa+1)/\{\Gamma(\kappa-\frac{1}{2})[\sqrt{\pi(\kappa+1)}]^3\}$. It has an asymptotic power-law dependence for large speed, x, and joins smoothly with a Maxwellian distribution at low speed.

The validation of the Kappa distribution with observations has been carried out by numerous researchers [37–40]. The rationalization of the Kappa distribution from different Fokker-Planck equations has also been considered [11,16,41,42]. Kappa distributions, occasionally referred to as the Student distribution, appear in mathematical applications of similar Fokker-Planck equations [43–46]. Shizgal has recently demonstrated that the particle distribution functions fitted to satellite data are not exactly Kappa distributions [47,48]. Dechant *et al.* [49] suggest a breakdown of Boltzmann-Gibbs statistical mechanics for confined laser-cooled atoms. The establishment of the nonequilibrium statistical mechanical behavior for these physical systems is an important endeavor.

The main objective of this paper is to provide a dynamical understanding of the physical origin of the Kappa distribution that arises primarily in space physics and other physical systems. Our goal is to provide a dynamical understanding of the formation of nonequilibrium distributions and the Kappa distribution in particular. We focus attention on the Fokker-Planck equations proposed by Biró and Jakovác [50], Borland [51], Lutz [52,53], Wada [54], and Wada *et al.* [55]. Borland [51] considers an FPE for which particular drift and diffusion coefficients yield either a Boltzmann distribution or a steady-state Kappa distribution, a result that arises from the inclusion of "*additive noise*" in the FPE. Likewise, Lutz proposes a FPE with particular drift and diffusion coefficients so as to model the motion of atoms in a one-dimensional optical lattice. For the appropriate choice of parameters, the steady distribution function is a Kappa distribution.

Shizgal [11] employed a FPE for charged particles of mass m interacting via Coulomb collisions with particles of mass M in large excess, that is

$$\frac{\partial f}{\partial t} = \frac{A}{v^2}\frac{\partial}{\partial v}\left[D_1(v)\left(1+\frac{kT_b}{mv}\frac{\partial}{\partial v}\right)\right]f(v,t) + \frac{B}{v^2}\frac{\partial}{\partial v}\left[v^2D_2(v)\frac{\partial f}{\partial v}\right], \quad v \in [0,\infty). \tag{4}$$

The normalization of $f(v)$ is $4\pi\int_0^\infty f(v,t)v^2dv = n$ in contrast to the one-dimensional Fokker-Planck equations, Eq. (6). The term in A corresponds to Coulomb collisions, the term in B to wave particle collisions, and Eq. (4) gives rise to non-Maxwellian distributions. The distribution function is clearly Maxwellian if $B = 0$, analogous to Eqs. (1) and (2), and non-Maxwellian for $B \neq 0$. For the particular choice of $D_2(v) \sim 1/v$ and for $m/M \to 0$, the steady distribution satisfies the Pearson ordinary differential equation,

$$\frac{df_\kappa(x)}{f_\kappa(x)} = -\left[\frac{2x}{1+\alpha x^2}\right]dx, \tag{5}$$

which defines the Kappa distribution, Eq. (3), where $\kappa = (1-\alpha)/\alpha$ where $\alpha = 2B/A$ [11]. It is important to point out that for finite m/M the distribution is not a Kappa distribution [41,56].

Although the Fokker-Planck operator in Eq. (4) corresponds to Coulomb collisions, the diffusion coefficient, $D_1(v)$, is evaluated without the contribution from large impact parameter collisions. Thus this system is not characterized by long-range collisions considered an important aspect for the origin of the Kappa distribution. Analogously, the previous works discussed above [50–53] for particular choices of the diffusion coefficients in the Fokker-Planck equations, Eq. (6) and Eq. (21), all yield a Pearson differential equation [11,16,41,42], Eq. (5), for the steady distribution that coincides with a Kappa distribution Eq. (3). It is clear that the Pearson differential equation, Eq. (5), yields a Kappa distribution for all α although the moments are not all finite for all α. For $\alpha \to 0$, that is, $\kappa \to \infty$, the distribution is a Maxwellian. The important question to be answered is the nature of the dynamical process that drives this system to a Kappa distribution or to a Maxwellian.

The purpose of this paper is to rationalize the occurrence of the Kappa distribution in different systems in terms of dynamical information in the Fokker-Planck equations rather than as arising from new statistical mechanics such as the Tsallis nonextensive entropy [57,58]. This follows on the work of previous papers [11,41,43,44,46–48]. We consider solutions of different Fokker-Planck equations with particular drift and diffusion coefficients [59].

Section II is a review of recent papers that purport to show that the occurrence of the Kappa distribution arises from "new physics" including nonextensive statistical mechanics. Section III describes the numerical method of solution of the FPE proposed by Chang and Cooper [60]. We consider in particular systems for which the steady distribution is close to but not exactly a Kappa distribution. We use the Fokker Planck equations reported by Biró and Jakovác [50], Lutz [52,53], and Wada [54]. There are also Fokker-Planck equations that arise in probability theory that result in the Student distribution [46] in finance and probability theory that we do not discuss.

Section IV presents detailed time-dependent solutions of the FPE based on the finite-difference solution reported by

Chang and Cooper [60]. We interpret the numerical results in terms of a spectral analysis of the FPE and the analogous Schrödinger equation. We show the behavior of the solutions of the FPE for systems for which the steady-state distribution is close to but not exactly a Kappa distribution. For these distributions, which cannot be rationalized in terms of the Tsallis nonextensive entropy, we provide a physical interpretation for their occurrence. Since these distributions are not far removed from the Kappa distribution, the physical basis for their occurrence is similar.

Section V is a summary of the main results which demonstrate that a variety of nonequilibrium effects arise from different famillies of Fokker-Planck equations. The class of nonequilibrium distributions studied in the current paper is only a small fraction of the many different nonequilibrium distributions in physics, chemistry, and astrophysics. There is no single entropic functional that can be used to validate these nonequilibrium distributions.

II. FOKKER-PLANCK EQUATIONS THAT YIELD MAXWELLIAN, KAPPA, AND OTHER DISTRIBUTIONS

Biró and Jakovać [50] considered the one-dimensional FPE of the form

$$\frac{\partial f(p,t)}{\partial t} = \frac{\partial}{\partial p}\left[-K_1(p)f(p,t) + \frac{\partial}{\partial p}K_2(p)f(p,t)\right],$$
$$p \in (-\infty, \infty), \tag{6}$$

with p and t dimensionless, and the drift and diffusion coefficients are modelled as polynomials, that is,

$$K_1(p) = F - Gp,$$
$$K_2(p) = D - 2Bp + Cp^2. \tag{7}$$

This FPE is defined by the coefficients B, C, D, F, and G without reference to a specific physical system. The steady-state distribution function of Eq. (6), $f_{ss}(p)$, subject to zero flux boundary condition is given by the Pearson differential equation [43–47],

$$\frac{d\ln f_{ss}(p)}{dp} = \frac{[K_1(p) - K_2'(p)]}{K_2(p)}. \tag{8}$$

The general FPE, Eq. (6), admits a large number of steady-state distributions dependent on the choice of the parameters. In contrast to the Fokker-Planck equations [Eqs. (1), (2), and (4)], the model FPE, Eq. (6), does not provide any explicit reference to a physical system of different particles in a heat bath at temperature T_b.

However, if we choose $B = C = F = 0$, $G = -1$, and in particular $D = mk_BT_b$, then the FPE given by Eq. (6) reduces to

$$\frac{\partial f(p)}{\partial t} = -2\frac{\partial}{\partial p}\left[pf(p) + \frac{k_BT_b}{m}\frac{\partial f(p)}{\partial p}\right], \qquad p \in (-\infty, \infty) \tag{9}$$

for which the steady distribution is the one-dimensional Maxwell distribution in momentum p, given by

$$f_{\max}(p) = \frac{1}{\sqrt{2\pi mk_B}}e^{-p^2/2mk_BT_b}, \tag{10}$$

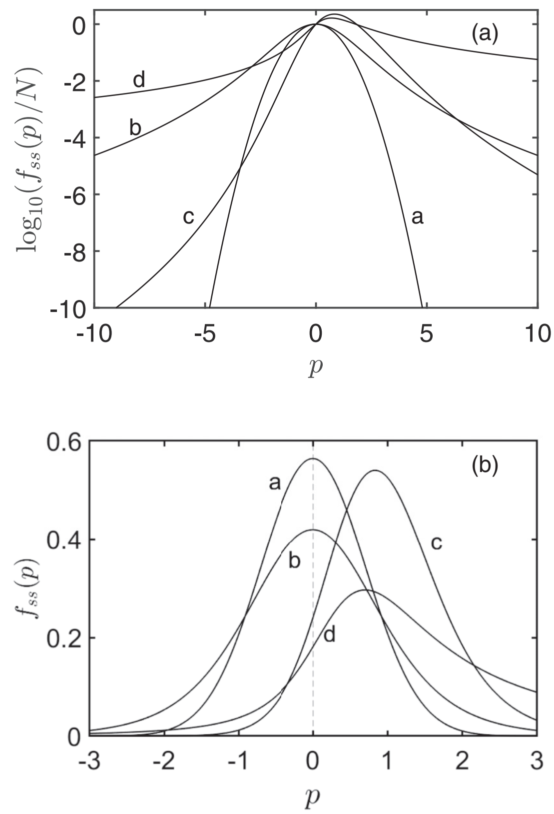

FIG. 1. Steady-state solutions of the Fokker Planck equation defined by Eqs. (6) and (7); a Symmetric Maxwellian: with $B = C = F = 0$, $D = 1$, $G = 2$; b Symmetric Kappa: with $B = F = 0$, $C = 0.2$ and $D = G = 1$, ($\kappa = 3.5$); c Assymetric nonequilibrium distribution: $B = 0$, $C = 0.2, D = 1$, $F = G = 2$; d Assymetric nonequilibrium distribution: $B = 0.2, C = D = F = 1, G = 0$.

and normalized according to

$$\int_{-\infty}^{\infty} f_{\max}(p)dp = 1. \tag{11}$$

In this way, we can identify the FPE, Eq. (9), with $D = mk_BT_b$, as for a test particle of mass m in a background at temperature, T_b, but this identification is arbitrary and not explicitly defined in Eq. (6) as in Eqs. (1) and (2).

However, with the choice $B = F = 0$ in Eq. (7), the steady distribution of Eq. (6) is given by the Pearson differential equation, Eq. (8) [44,45,47], and we have that

$$\frac{d\ln f_{ss}(p)}{dp} = -\frac{(G+2C)p}{D+Cp^2}. \tag{12}$$

If we set $p = xp_{\text{th}}$, and identify $p_{\text{th}}^2 = 2D/(2C+G)$ and $\alpha = D/Cp_{\text{th}}^2$, then we have that

$$\frac{d\ln f_{ss}(p)}{dp} = -\frac{2x}{1+\alpha x^2}, \tag{13}$$

analogous to the definition of the κ distribution in Ref. [11]. Thus, the steady distribution, Eq. (12), can be written as the Kappa distribution

$$f_\kappa(p) = C(\kappa)\left(1 + \frac{1}{\kappa}\frac{p^2}{p_{\text{th}}^2}\right)^{-\kappa}, \tag{14}$$

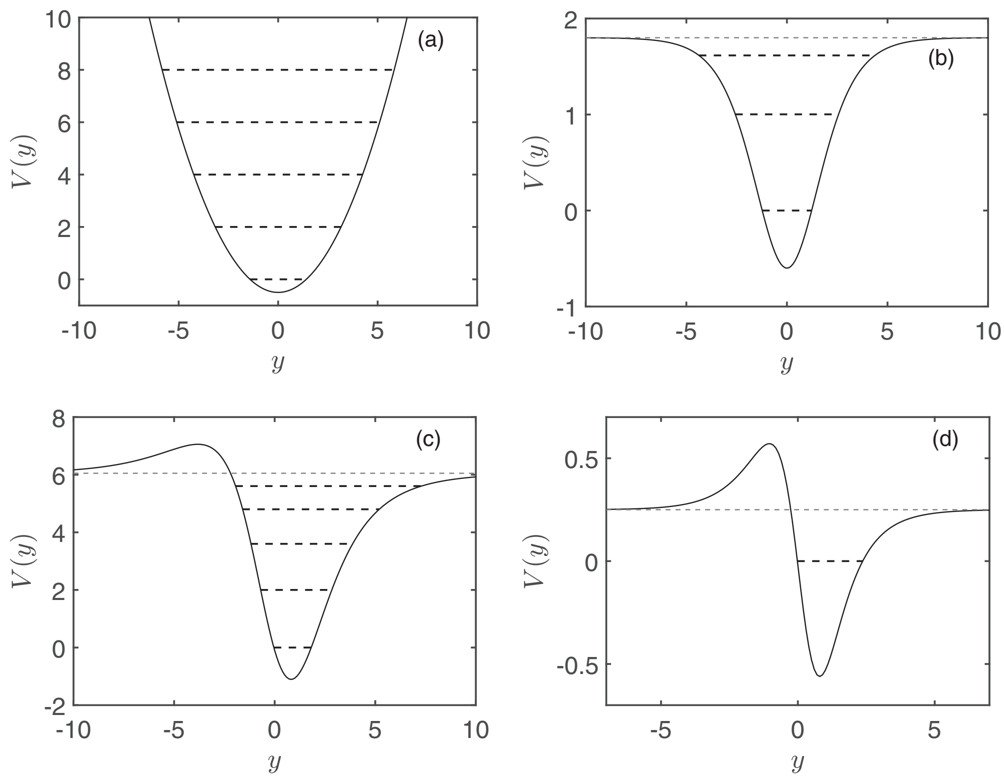

FIG. 2. Potential functions, $V(y)$, in the Schrödinger equation corresponding to the Fokker-Planck equation, Eq. (6), with (a) $F = B = C = 0$, $G = 2$, and $D = 1$; (b) $F = B = 0$, $G = D = 1$ and $C = 0.2$; (c) $F = G = 2$, $D = 1$, $B = 0$, and $C = 0.2$; dashed lines denote the bound eigenvalues.

where $\alpha = 1/\kappa$ and $C(\kappa) = \int_{-\infty}^{\infty} f_\kappa(p)p^2 dp$ is the normalization of the distribution function.

An important result of the current work is the observation that in addition to the Maxwellian and Kappa distributions, the FPE, Eq. (6), with the drift and diffusion coefficients defined by Eq. (7), defines a very large family of nonequilibrium distributions. With $G = 0$, the general steady solution of the FPE, Eq. (6), has the analytic solution [61]

$$f_{\rm ss}(p) = N(Cp^2 - 2Bp + D)^{-1} \times \exp\left[\frac{F}{\sqrt{CD - B^2}} \tan^{-1}\left(\frac{Cp - B}{\sqrt{CD - B^2}}\right)\right]. \tag{15}$$

For $B = 0$, Eq. (8) gives

$$f_{\rm ss}(p) = N\left(1 + \frac{C}{D}p^2\right)^{-(1+G/2C)} \exp\left[\frac{F}{\sqrt{CD}} \tan^{-1}\left(\sqrt{\frac{C}{D}}p\right)\right], \tag{16}$$

where $N = \int_{-\infty}^{\infty} f_{\rm ss}(p)e^{-p^2} dp$ is the normalization. It is clear that the FPE proposed by Biró and Jakovác [50] possesses a large family of nonequilibrium distributions in addition to a Maxwellian, Eq. (10), and the Kappa distribution, Eq. (14). The Tsallis maximum entropy formalism [62] only rationalizes the Kappa distribution. In Fig. 1(a), we show four steady distributions of Eq. (6) as $\log_{10}[f_{\rm ss}(p)/N]$ for which a is a Maxwellian and b is a Kappa distribution. For other choices of the parameters, we show with the curves c and d examples of asymmetric distributions that are neither Maxwellian nor Kappa distributions. These distributions cannot be rationalized in terms of a maximum entropy principle.

Following the work of Stariolo [63] and Borland [51], Lutz [52,53] employed the FPE equation,

$$\frac{\partial W(p)}{\partial t} = -\frac{\partial}{\partial p}\left\{K(p)W(p) + \frac{1}{2}\frac{\partial}{\partial p}[D(p)W(p)]\right\}, \quad p \in (-\infty, \infty), \tag{17}$$

analogously to Eq. (6) with drift and diffusion coefficients $K(p)$ and $D(p)$ given by

$$K(p) = -\frac{\alpha p}{1 + (p/p_c)^2}, \tag{18}$$

$$D(p) = D_0 + \frac{D_1}{1 + (p/p_c)^2}.$$

The steady-state distribution of Eq. (17) with the coefficients Eq. (18) is given by

$$\frac{d\ln[W_{\rm ss}(p)]}{dp} = \frac{-\alpha p}{(D_0 + D_1) + D_0\left(p^2/p_c^2\right)}, \tag{19}$$

and the steady-state distribution is

$$W_{\rm ss}(p) = N\left[1 + \frac{D_0}{D_0 + D_1}\frac{p^2}{p_c^2}\right]^{\frac{-\alpha p_c^2}{2D_0}}. \tag{20}$$

This yields either the Maxwellian distribution, Eq. (10), with $D_0 = 0$ and $D_1 = 1$ or the Kappa distribution, Eq. (14), with $D_0 = 1$ and $D_1 = 0$. Equation (19) also gives a Maxwellian for $p_c \to \infty$.

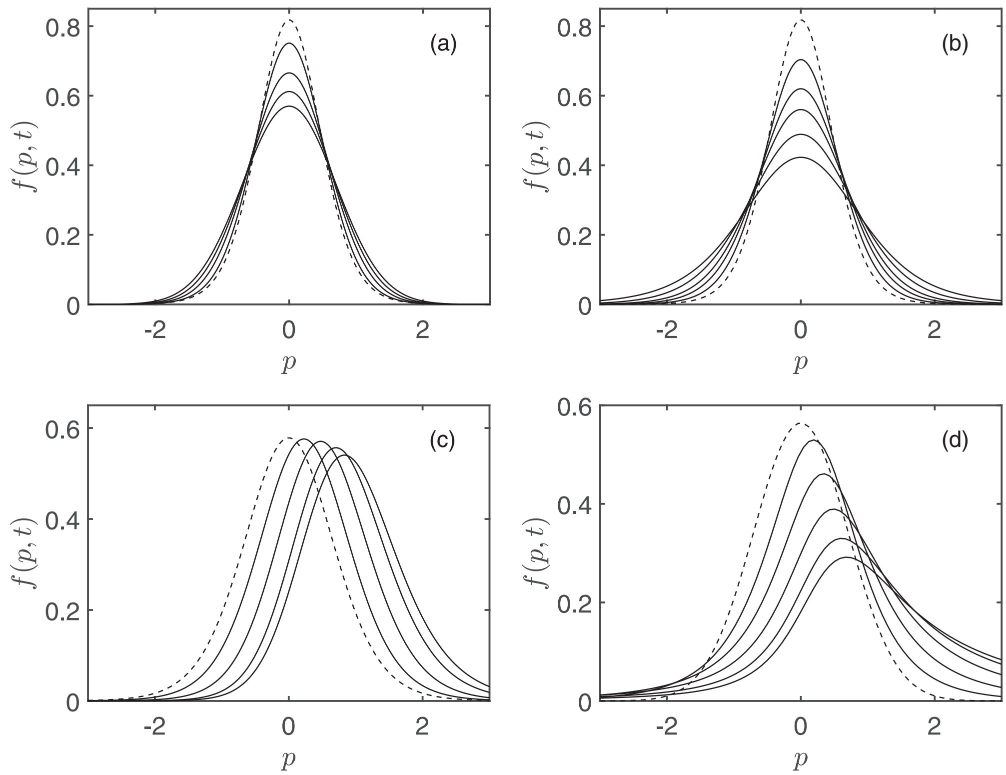

FIG. 3. Time evolution of the distribution function for the FPE, Eq. (6), with the constants in Eq. (6) as in Fig. 1 for an initial Maxwellian (dashed curve) and different steady states as shown in Fig. 1(b). Successive dimensionless times increase from top to bottom curves. (a) $f(p,0)=\sqrt{\frac{3}{2\pi}}e^{-3/2p^2}$, FPE with $B=C=F=0$, $D=1$, $G=2$; steady-state Maxwellian, Eq. (10), $t=0$, 0.05, 0.15, 0.30, and 0.80. (b) $f(p,0)=\frac{1}{\sqrt{\pi}}e^{-p^2}$, FPE with $B=F=0$, $C=0.2$, $D=G=1$; steady-state Kappa distribution ($\kappa=3.5$), Eq. (12), $t=0$, 0.07, 0.15, 0.25, 0.5, and 2. (c) $f(p,0)=\frac{1}{\sqrt{\pi}}e^{-p^2}$, FPE with $B=0$, $C=0.2$, $D=1$, $F=G=2$; steady state is given by Eq. (15), $t=0$, 0.15, 0.40, 0.90, and 3.0. (d) $f(p,0)=\frac{1}{\sqrt{\pi}}e^{-p^2}$, FPE with $B=0.2$, $C=D=F=1$, $G=0$; steady state is given by Eq. (16), $t=0$, 0.15, 0.40, 0.90, 2.0, and 5.0.

Wada [54] employed a FPE of the form

$$\frac{\partial W^{(n)}(p,t)}{\partial t}=-\frac{\partial}{\partial p}[K_n(p)W^{(n)}(p,t)]+\frac{\partial}{\partial p}\left[D(p)\frac{\partial W^{(n)}(p,t)}{\partial p}\right],\quad p\in(-\infty,\infty), \tag{21}$$

with drift and diffusion coefficients defined by

$$K_n(p)=\frac{-\alpha p}{\left[1+p^{2n}/p_c^{2n}\right]^{1/n}},\qquad D(p)=D_0+\frac{D_1}{1+p^2/p_c^2}, \tag{22}$$

parametrized with an additional integer parameter n. For $n=1$, this corresponds to the FPE, Eq. (17), so that $W_{\rm ss}^{(1)}(p)\equiv W_{\rm ss}(p)$, Eq. (20). The steady-state distribution subject to zero flux boundary conditions is given by the Pearson differential equation,

$$\frac{d\ln W_{\rm ss}^{(n)}(p)}{dp}=\frac{K_n(p)}{D(p)}. \tag{23}$$

One aspect of this model is that in the limit $n\to\infty$ the variation of the drift coefficient with p changes abruptly from linear in p to inversely with p, that is,

$$K_{n\to\infty}(p)\to\begin{cases}-\alpha p & |p|\leqslant p_c,\\ -\alpha p_c^2/p & |p|\geqslant p_c.\end{cases} \tag{24}$$

Wada [54] considered the case $n=2$ and $D_1=0$ for which the steady-state distribution is given by the Pearson differential equation

$$\frac{d\ln[W_{\rm ss}^{(2)}(p)]}{dp}=\frac{-\alpha p}{D_0\sqrt{1+(p^4/p_c^4)}}. \tag{25}$$

Thus we have that

$$W_{\rm ss}^{(2)}(p)=N_2\exp\left[\frac{-\alpha p_c^2}{2D_0}\sinh^{-1}\left(p^2/p_c^2\right)\right]. \tag{26}$$

On the other hand, for the drift coefficient, $K_n(p)$, Eq. (24), with $n=2$ and $D_1\neq 0$, we get the steady-state solution with the additional term in D_1,

$$\ln\left(W_{\rm ss}^{(2)}(p)/N_2\right)=\frac{-\alpha p_c^2}{2D_0}\left[\sinh^{-1}\left(p^2/p_c^2\right)+\frac{D_1}{\theta}\tanh^{-1}\left(\frac{D_0-\frac{D_0+D_1}{p_c^2}p^2}{\theta\sqrt{1+p^2/p_c^2}}\right)\right], \tag{27}$$

where $\theta=\sqrt{2D_0^2+2D_0D_1+D_1^2}$.

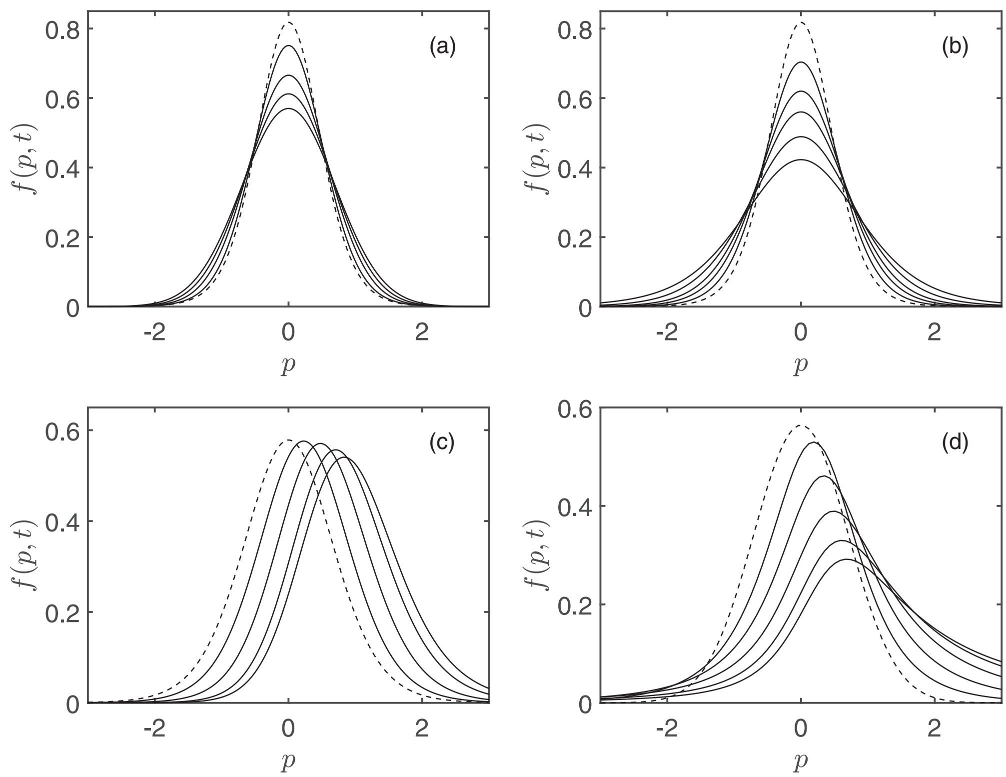

FIG. 4. Time evolution of the distribution function, $f(p,t)$, for the FPE, Eq. (6), with the initial Kappa distribution $f(p,0) = N(1 + p^2/5)^{-5}$, dashed curve; for dimensionless time, t, which increases from top to bottom curves; the steady distributions are (a) Maxwellian; $t = 0.05$, 0.15, 0.30, and 0.80. (b) Kappa distribution shown by the curve b in Fig. 1(b); $t = 0.05$, 0.15, 0.25 0.30, and 0.80. (c) Asymmetric distribution c in Fig. 1(b); $t = 0.07$, 0.15, 0.50, and 2.0. (d) Asymmetric distribution d in Fig. 1(b); $t = 0.15$, 0.40, 0.90 2.0, and 3.0.

We also consider the solution for arbitrary n and the steady-state distribution is given in terms of the integral,

$$W_{\rm ss}^{(n)}(p) = -N_n \exp\left\{\int_0^p -\frac{\alpha\xi\left(\xi^2+p_c^2\right)[1+(\xi/p_c)^{2n}]^{1/n}}{(D_0+D_1)p_c^2+D_0\xi^2}d\xi\right\}, \tag{28}$$

where the normalization is defined by

$$N_n = 4\pi\int_0^\infty W_{\rm ss}^{(n)}(p)p^2 dp, \tag{29}$$

which can be evaluated numerically. Thus the FPE, Eq. (21), with drift and diffusion coefficients given by Eq. (22), possesses a myriad of nonequilibrium distributions which are not necessarily Kappa or Maxwellian distributions. Additional modifications to this model were reported by Wada *et al.* [55] with the further demonstration of the vast number of nonequilibrium distributions that arise from the FPE in addition to the Maxwellian and Kappa distributions. A detailed comparison of these distributions is presented and discussed in Sec. V.

III. SPECTRAL SOLUTION OF THE FPE AND THE RELATIONSHIP TO THE SCHRÖDINGER EQUATION

The linear FPE, Eq. (6) for $f(p,t)$, admit solutions in terms of the eigenfunctions and eigenvalues of the self-adjoint Fokker-Planck operators defined by Eq. (6) and denoted by L. Thus we can define the real eigenvalues λ_k, and the eigenvectors, $\phi_k(x)$, of L, with the eigenvalue problem,

$$L\phi_k(x) = \lambda_k\phi_k(x). \tag{30}$$

The solution to the time-dependent FPE can be expressed as

$$f(x,t) = \sum_{k=0}^{\infty} c_k\phi_k(x)e^{-\lambda_k t}, \tag{31}$$

where c_k are determined with the initial distribution $f(x,0)$. Since the Fokker-Planck operator is self-adjoint, the eigenvalues are real and the solution evolves exponentially in time.

The FPE, Eq. (6), can be transformed to a Schrödinger equation with the transformation,

$$\begin{aligned} y(p) &= \int^p \frac{1}{\sqrt{K_2(p')}}\,dp', \\ &= \frac{1}{\sqrt{C}}\left(\sinh^{-1}\left[\frac{Cp-B}{\theta}\right] + \sinh^{-1}\left[\frac{B}{\theta}\right]\right), \end{aligned} \tag{32}$$

where $\theta = \sqrt{CD-B^2}$. This transformation of a Fokker-Planck eigenvalue problem leads to a Schrödinger equation in the class of supersymmetric quantum mechanics [64,65] so that the potential is of the form

$$V(y) = \left(\frac{dC}{dy}\right)^2 - \frac{d^2C}{dy}, \tag{33}$$

where

$$C(y) = -\frac{1}{2}\int^y \frac{K_1[p(y')]}{\sqrt{K_2 p(y')}}dy' + \frac{1}{4}\log[K_2[p(y)]]. \tag{34}$$

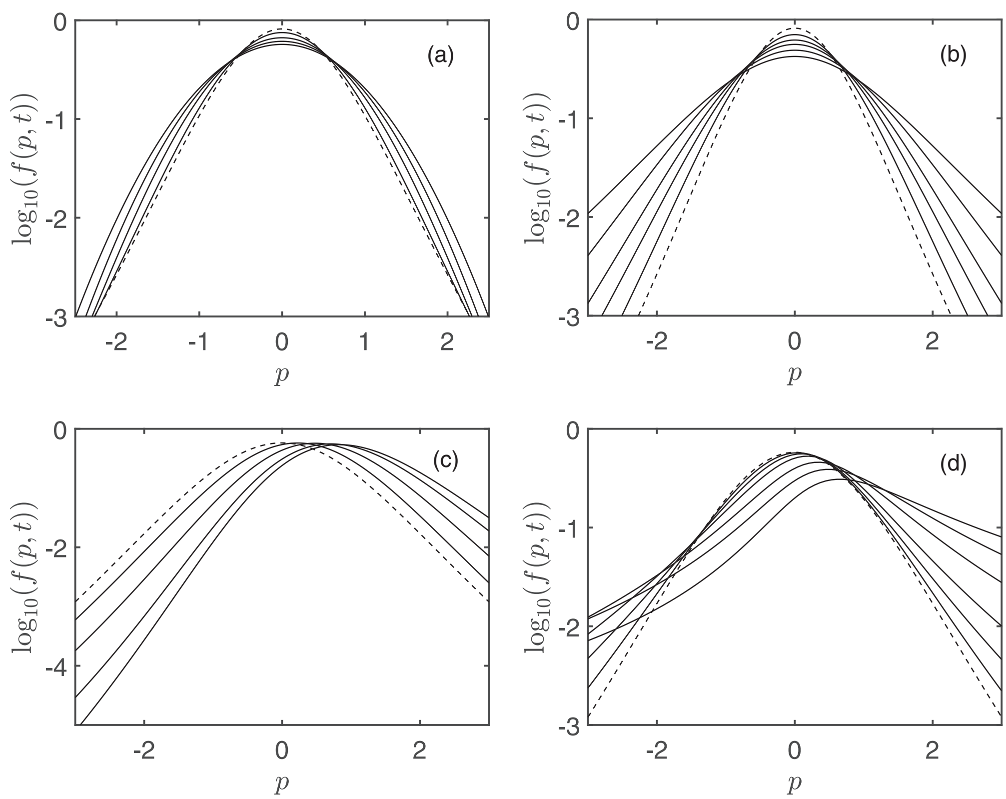

FIG. 5. Time evolution of the distribution function, $\log_{10}[f(p,t)]$ for the FPE in Eq. (6) for an initial Kappa distribution, $f(p,0) = N(1+\frac{2p^2}{5})^{-5}$, and different steady states analogous to Fig. 4. Successive times, t, increases from top to bottom curves. (a) Steady Maxwellian Eq. (10); $t = 0$, 0.05, 0.15, 0.3, and 0.8. (b) Steady Kappa distribution, Eq. (14); $t = 0$, 0.07, 0.15, 0.25, 0.5, and 2. (c) Steady nonequilibrium distribution, Eq. (16); $t = 0$, 0.15, 0.4, 0.9, and 3. (d) Steady nonequilibrium distribution, Eq. (15); $t = 0$, 0.15, 0.4, 0.9, 2, and 5.

This gives the Schrödinger equation isospectral with the FPE, that is,

$$-\frac{d^2\phi_n}{dy^2} + V(y)\phi_n = \lambda_n\phi_n. \tag{35}$$

This provides a useful interpretation for the time-dependent solutions of the Fokker-Planck equations in terms of the eigenvalue spectrum. The potentials in the Schrödinger equation corresponding to the FPE, Eq. (6), are shown in Fig. 2 for several system parameters. It is clear the the spectral properties vary considerably with the system parameters. The eigenvalue spectrum shown in Fig. 2(a) is entirely discrete, whereas for the other system parameters in Figs. 2(b)–2(d) there exist a finite number of bound states and a continuum. In particular, for the system parameters in Fig. 2(a), there is only the zero eigenvalue associated with the steady distribution and the remainder of the eigenvalues are in the continuum. A similar analysis of the spectral properties of the Schroedinger equation associated with the FPE proposed by Wada, Eq. (21), can also be carried out.

Although a spectral method could be used for these systems, the Chang-Cooper algorithm [60] is more efficient. The convergence of the eigenvalue and eigenfunction representation of the time-dependent solution, Eq. (31), can be slow owing to the continuum in the eigenvalue spectrum [46,56,59]. As a consequence, the time-dependent solutions are obtained with the Chang-Cooper algorithm [60] discussed in the next section. The details of the potential functions, shown in Fig. 2, provide a useful interpretation of the spectral properties of the Fokker-Planck operator.

IV. TIME-DEPENDENT DISTRIBUTIONS AND THE DYNAMICAL ORIGIN OF NONEQUILIBRIUM AND KAPPA DISTRIBUTIONS; THE KULLBACK-LEIBLER ENTROPY

The time-dependent Fokker-Planck equations, Eq. (6) for $f(p,t)$ and Eq. (21) for $W^{(n)}(p,t)$, are solved with a finite-difference scheme introduced by Chang and Cooper [60] and used previously [56,66]. This is modified here for application to the 1D Fokker-Planck equations. We set $t_n = n\Delta t$ and use a backward Euler difference for the time derivative, that is,

$$\frac{\partial g(x_i,t_n)}{\partial t} = \frac{g_i^{n+1} - g_i^n}{\Delta t},$$
$$= \frac{D_{i+1}B_{i+1}\left(g_{i+1}^{n+1} - g_i^{n+1}\right) - D_iB_i\left(g_i^{n+1} - g_{i-1}^{n+1}\right)}{(\Delta x)^2 D_{i+1/2}}, \tag{36}$$

where $g(x,t)$ is defined in terms of the distribution functions as $f(p,t) = f_{\max}(p)g(p,t)$ [see Eq. (6)] or which after rearranging terms can be written as

$$\sum_{j=1}^{N} V_{ij}g_j^{n+1} = g_i^n, \tag{37}$$

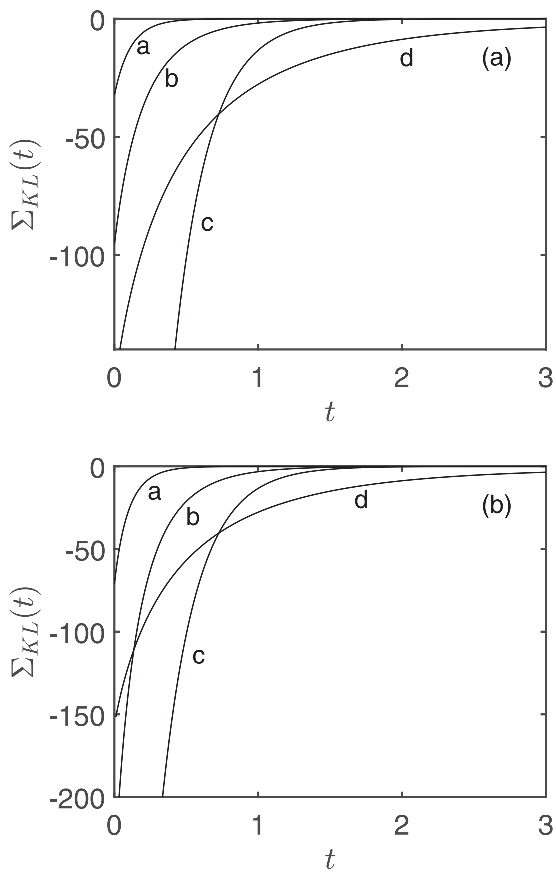

FIG. 6. Time dependence of the Kullback-Leibler entropy, Eq. (41). (a) Time-dependent distributions in Fig. 3. (b) time-dependent distributions in Fig. 4. Steady states for the curves are given by a Eq. (10), b Eq. (12), c Eq. (16), and d Eq. (15).

where V is a tridiagonal matrix, that is,

$$\begin{aligned} V_{ii} &= 1 + \Delta t L_{i,i}, \quad i = 1, \ldots, N, \\ V_{i,i-1} &= \Delta t L_{i,i-1}, \quad i = 2, \ldots, N, \\ V_{i,i+1} &= \Delta t L_{i,i+1}, \quad i = 1, \ldots, N-1. \end{aligned} \tag{38}$$

The discretized version of Eq. (36) becomes

$$\frac{g_i^{n+1} - g_i^n}{\Delta t} = L_{ij} g_j^{n+1}. \tag{39}$$

This results in the following implicit scheme for the time evolution of the distribution function:

$$g_i^{n+1} = \sum_{i=1}^{N} [\delta_{ij} - \Delta t L_{ij}]^{-1} g_i^n. \tag{40}$$

We consider time-dependent solutions of the model Fokker-Planck equations reported by Biro and Jakovac [50] with coefficients defined with Eq. (6), by Lutz [52] with coefficients defined by Eq. (18), and by Wada [54], Eq. (21), with coefficients defined by Eq. (22) so as to clarify the dynamics of the establishment of nonequilibrium distributions and the Kappa distribution in particular. This follows on the earlier work by Zhang and Shizgal [56]. We choose parameters in the respective Fokker-Planck equations that yield Kappa distributions as well as parameters that yield other nonequilibrium distributions. The main objective is to clarify the physical mechanisms that create the different nonequilibrium distributions.

There have been numerous discussions regarding the physical origin of the Kappa distribution, primarily in space physics and also concerning optical lattices. There have been many authors who base the origin of the Kappa distribution on the extremum of the Tsallis nonextensive entropy functional [15,38,39,46,50,53,57,67–69], to list a few. On the other hand, it has been demonstrated that the Kappa distribution (analogous to the Student distribution [43–47]) arises as the steady distribution of a FPE as given by a Pearson differential equation for very specific system parameters. For slightly different parameters in the FPE, the distribution functions depart from the Kappa distribution and the Tsallis nonextensive entropy formalism plays no role.

We consider the time-dependent solutions of the FPE, Eq. (6), for a choice of parameters in Eq. (7) that give a steady-state distribution that is either a Maxwellian, Eq. (10), or a Kappa distribution, Eq. (14), and a distribution that is neither a Maxwellian nor a Kappa distribution. The initial distribution is the Maxwellian with a particular temperature.

The time-dependent solutions of the Biró-Jakovać FPE [50], Eq. (6), were obtained with the Chang-Cooper algorithm [60] and are shown in Figs. 2–4 for either an initial Maxwellian or an initial Kappa distribution. In Fig. 3, the time evolution of the distribution functions given by the solution of the FPE, Eq. (6), for an initial Maxwellian (dashed curve) are shown for different constants, B, C, D, F, and G, that define the drift and diffusion coefficients in Eq. (7). The nonequilibrium steady-state distributions in Fig. 3 are shown as in Fig. 1, curves a–d. The steady-state distribution in Fig. 3(b) is the Kappa distribution.

In Fig. 3, the time evolution of the distribution functions given by the solution of the Biro-Jakovac FPE, Eq. (6), for an initial Maxwellian distribution (dashed curve) is shown for different constants, B, C, D, F, and G, that define the drift and diffusion coefficients, in Eq. (7). Figure 3(a) shows the time evolution of the initial Maxwellian distribution to a Maxwellian at a different temperature, whereas Fig. 3(b) shows the time evolution of an initial Maxwellian distribution to a steady-state Kappa ($\kappa = 3.5$). Figures 3(c) and 3(d) show the time evolution of the initial Maxwellian distribution to nonequilibrium asymmetric distributions, Eqs. (15) and (16), that are neither Maxwellian nor Kappa distributions.

In Fig. 4, the time evolution of the distribution functions given by the solution of the Biro-Jakovac FPE, Eq. (6), for an initial Kappa distribution (dashed curve) is shown for different constants, B, C, D, F, and G, that define the drift and diffusion coefficients in Eq. (7). Figure 4(a) shows the time evolution of the initial Kappa distribution ($\kappa = 5$) to a Maxwellian, whereas Fig. 4(b) shows the time evolution of an initial Kappa distribution ($\kappa = 5$) to a steady-state Kappa ($\kappa = 3.5$). Figures 4(c) and 4(d) show the time evolution of the initial Kappa distribution to asymmetric nonequilibrium distributions.

In Fig. 5, the distributions in Fig. 4 are redrawn as $\log_{10}[f(p,t)]$ so as to show the behavior of the *tails* of the

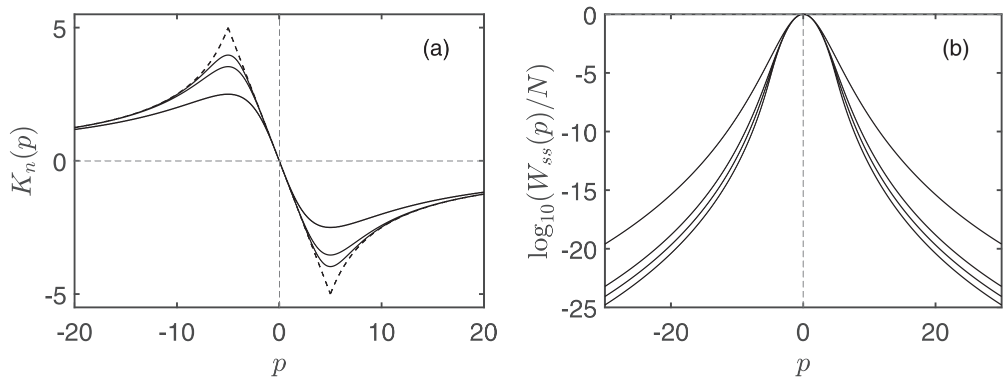

FIG. 7. (a) Drift coefficient $K_n(p)$ in Eq. (21) [54] with $D_0 = D_1 = \alpha = 1$ and $p_c = 5$; dashed line is for $n \to \infty$; and subsequent lines are for $n = 1$, 2 and 3. (b) The steady distribution $\log_{10}[W_{ss}^{(n)}(p)/N]$ for $n = 1$, 2, 3, and 10 from top to bottom curves.

distribution as $p \to \pm\infty$. There is a clear contrast of this behavior for the distributions in Figs. 5(c) and 5(d) with a distinctive assymetric behavior in contrast with the symmetric distributions in Figs. 5(a) and 5(b). This serves to emphasize that the Fokker-Planck equations can yield families of distributions that are neither Maxwellian nor Kappa distributions and the usual maximum entropy variational methods based on either Boltzmann-Gibbs entropy or Tsallis nonextensive entropy do not apply.

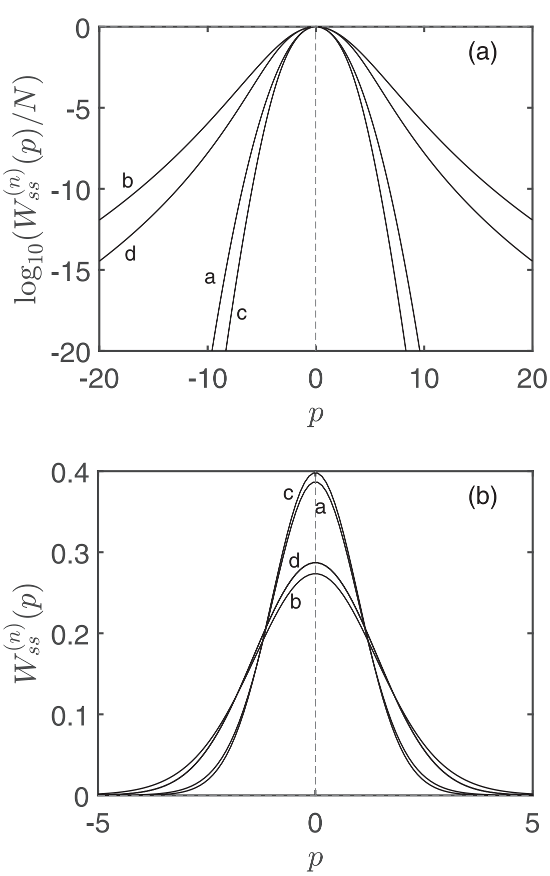

FIG. 8. Steady-state solutions, $W_{ss}^{(1)}(p)$, Eq. (20) and $W_{ss}^{(2)}(p)$, Eq. (26) with drift and diffusion coefficients Eq. (22); $p_c = 5$, $D_1 = \alpha = 1$ and a $n = 1$, $D_0 = 0$; b $n = 1$, $D_0 = 1$; c $n = 2$, $D_0 = 0$; d $n = 2$, $D_0 = 1$.

It is the Kullback-Leibler divergence defined by

$$\Sigma_{\rm KL}(t) = -\int_{-\infty}^{\infty} f(x,t) \ln\left[\frac{f(x,t)}{f_{\rm ss}(x)}\right] dx, \qquad (41)$$

that measures the departure of an arbitrary distribution, $f(x,t)$, from the steady-state distribution, $f_{\rm ss}(x)$ [70]. The Kullback-Leibler divergence does not provide the nonequilibrium distribution but serves to show the approach to a steady nonequilibrium state. We show in Fig. 6(a) the time evolution of $\Sigma_{\rm KL}(t)$ for the time-dependent solutions shown in Fig. 3. Figure 6(b) shows $\Sigma_{\rm KL}(t)$ for the time-dependent distributions of Fig. 4. The Kullback-Leibler divergence varies monotonically with time from some initial negative value determined by the initial distribution to zero.

Lutz [52,53] introduced the FPE, Eq. (17), with the drift and diffusion coefficients defined by Eq. (18) with the four parameters α, x_c, D_0, and D_1 which gives only the Maxwellian and Kappa steady distributions as noted earlier. On the other hand, Wada [54] introduced the modified form, Eq. (21), with the steady distribution Eq. (23) with the modified drift and diffusion coefficients given by Eq. (22). In Fig. 7(a), we show the variation of the coefficient, $K_n(p)$, in the FPE, Eq. (21), proposed by Wada [54] for $n = 1$, 2, and 3. The steady-state distributions of this FPE, $\log_{10}[W_{ss}(p)/N]$, exhibit extended high-energy "tails" as shown in Fig. 7(b). These nonequilibrium distributions are neither Maxwellian nor Kappa distributions. This demonstration is further evidence that there exists vast numbers of different particle distributions as the steady solutions of a FPE that are neither Maxwellian nor Kappa distributions. These distributions are not derivable from any maximum entropy variational principle.

In Fig. 8, the steady-state nonequilibrium distribution functions from the Wada FPE, Eq. (21), are shown with $p_c = 5$, $D_1 = \alpha = 1$ versus n and D_0. The objective is to show the variety of nonequilibrium distributions that are neither Maxwellian nor Tsallis entropy-derived Kappa distributions. The variation of these nonequilibrium distributions is shown in Fig. 8 versus the remaining parameters n (either 1 or 2) and D_0 (either 0 and 1). In Fig. 8(a), we compare the behavior of $\log_{10}[W_{ss}^{(n)}(p)/N]$ for $n = 1$

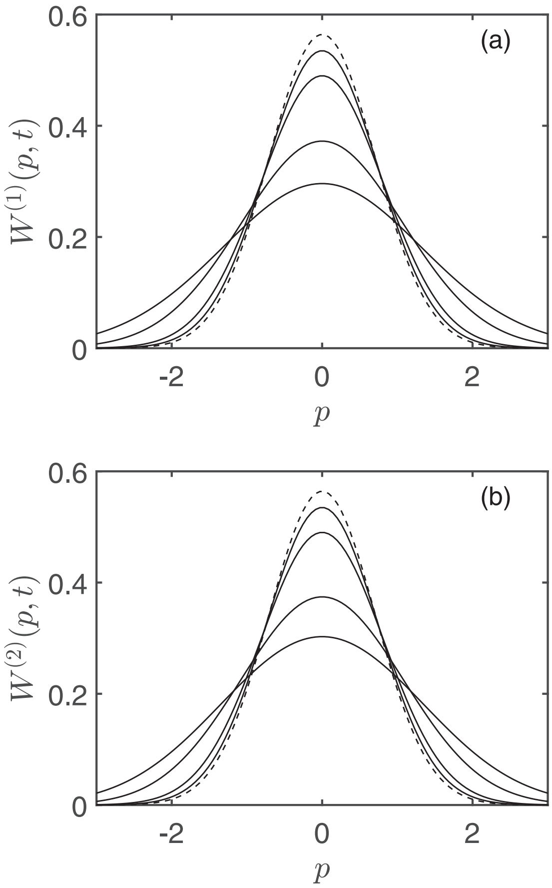

FIG. 9. Time evolution of the distribution function, $W^{(n)}(p,t)$, given by the FPE in Eq. (23) for an initial Maxwellian $W(p,0) = \frac{1}{\sqrt{\pi}}e^{-p^2}$ and with $K_n(p)$ and $D(p)$ defined by Eq. (22). Successive times in units of α^{-1} and increase from top to bottom curves and are $t = 0$, 0.03, 0.07, 0.3, and 1; the dashed curves are the initial distributions (a) The Maxwellian is given by Eq. (25) (Kappa); see the caption to Fig. 8(b). (b) Nonequilibrium distribution with $D_0 = D_1 = \alpha = 1$, $p_c = 5$, $n = 2$, and $t = 0$, 0.03, 0.07, 0.3, and 1.

(curve b) with $n = 2$ (curve d) for $D_0 = 1$. These results demonstrate the existence of distributions with extended tails analogous to Kappa distributions. This behavior is compared with curves a ($n = 1$) and b ($n = 2$) for $D_0 = 0$ which is analogous to a Maxwellian distribution. The distributions in Fig. 8(a) are replicated in Fig. 8(b) on a linear rather than logarithmic scale.

In Fig. 9, we show the time-dependent evolution of the distribution functions, $W^{(n)}(p,t)$, for $n = 1$ [Fig. 9(a)] and $n = 2$ [Fig. 9(b)] defined by the Wada FPE, Eq. (21), with coefficients $K_n(p)$ and $D(p)$. The steady distributions are neither Maxwellian nor Kappa distributions. We show the approach to these nonequilibrium distributions in terms of the time-dependent Kullback-Leibler divergence, $\Sigma_{\rm KL}(t)$, Eq. (41), identified as a for Fig. 10(a) and b for Fig. 10(b).

V. SUMMARY

In this paper, we have provided a detailed analysis of the nonequilibrium behavior of different model systems as described by a variety of Fokker-Planck equations. The phenomena studied include the physical origin of the Kappa distribution that has been proposed by numerous authors as the almost universal distribution for energetic particles in the heliosphere [15,37,39,47,48,58] and in the physics of optical lattices [50–53,71]. The main thrust of the present work is the demonstration that these systems, as described with Fokker-Planck equations, can have numerous nonequilibrium distributions, not necessarily the Kappa distribution which is uniquely provided with the Tsallis nonextensive formalism. The Kappa distributions for these systems arise only for a particular set of system parameters that define the drift and diffusion coefficients in the Fokker-Planck equations. A different set of nonequilibrium distributions are obtained for different choices of these system parameters however close to the parameter values that yield the Kappa distribution. The steady distributions that arise from the Fokker-Planck equations are defined in terms of the Pearson (ordinary) differential equation which can provide distribution functions with asymptotic power-law distributions [43–45]. The bimodal distributions of electrons in the inert gas moderators with deep Ramsauer-Townsend minima [72,73] are not derivable from a maximum entropy formalism. These nonequilibrium distributions arise owing to the functional form of the particular drift and diffusion coefficents in the FPE. There is no new fundamental entropic functional required to rationalize these distributions.

A review of the wide range of systems studied with the theoretical methods in nonequilibrium statistical mechanics was briefly provided in the Introduction with reference to the Boltzmann, Fokker-Planck, and Master equations [5,6,8,9,22,23,25,60] applied to classical and quantum systems for both neutral and charged particles. These theoretical descriptions of systems out of equilibrium from a particle description are complemented with the methods of irreversible thermodynamics [7,18,32] analogously to stochastic thermodynamics [19–21]. In the current paper, Fokker-Planck equations were studied with different drift and diffusion coefficients. The steady-state nonequilibrium distributions are given by the Pearson ordinary differential equations, Eqs. (5), (8), (12), and (23), which are in effect detailed balance conditions. There is no known entropy functional that can provide these nonequilibrium distributions.

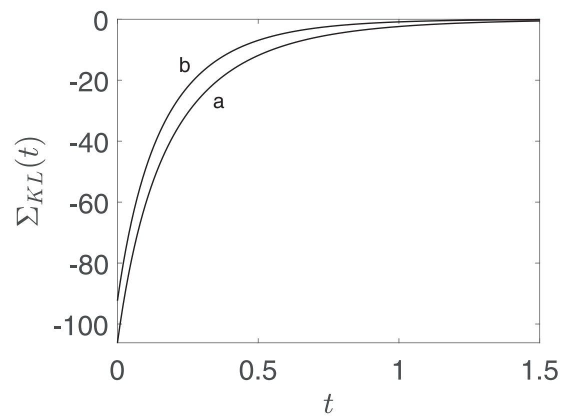

FIG. 10. Time dependence of the Kullback-Leibler entropy, $\Sigma_{\rm KL}(t)$, Eq. (42), for the distributions in Fig. 9; curve a for 9(a) and curve b for 9(b).

ACKNOWLEDGMENT

This research was supported by a grant to Bernard Shizgal by the National Science and Engineering Research Council of Canada (Research Grant No. GR03913). A.D.O. was supported in part with a UBC Work Learn International Undergraduate Research Award. We are grateful to Yin Huang for useful discussions.

[1] I. Prigogine and E. Xhrouet, On the perturbation of Maxwell distribution function by chemical reactions in gases, Physica **15**, 913 (1949).

[2] J. Ross and P. Mazur, Some deductions from a formal statistical mechanical theory of chemical kinetics, J. Chem. Phys. **35**, 19 (1961).

[3] B. Shizgal and M. Karplus, Nonequilibrium contributions to the rate of reaction. I. Perturbation of the velocity distribution, J. Chem. Phys. **52**, 4262 (1970).

[4] R. Brun, *Introduction to Reactive Gas Dynamics* (Oxford University Press, Oxford, 2009).

[5] E. W. Montroll and K. E. Shuler, Studies in nonequilibrium rate processes. I. The relaxation of a system of harmonic oscillators, J. Chem. Phys. **26**, 454 (1957).

[6] M. Capitelli (ed.), *Nonequilibrium Vibrational Kinetics* (Springer Verlag, Berlin, 1986).

[7] N. G. Van Kampen, *Stochastic Processes in Physics and Chemistry*, 3rd ed. (Elsevier, Amsterdam, 2007).

[8] M. M. R. Williams, *Mathematical Methods in Particle Transport Methods* (Butterworths, London, 1971).

[9] B. Davison and J. B. Sykes, *Neutron Transport Theory* (Oxford University Press, Oxford, 1957).

[10] W. C. Feldman, J. R. Asbridge, S. J. Bame, M. D. Montgomery, and S. P. Gary, J. Geophys. Res. **80**, 4181 (1975).

[11] B. D. Shizgal, Suprathermal particle distributions in space physics: Kappa distributions and entropy, Astrophys. Space Sci. **312**, 227 (2007).

[12] S. Kim, P. H. Yoon, G. S. Choe, and L. Wang, Asymptotic theory of solar wind electrons, Astrophys. J. **806**, 32 (2015).

[13] M. Lazar, H. Fichtner, and P. H. Yoon, On the interpretation and applicability of κ-distributions, Astron. Astrophys **589**, A39 (2016).

[14] V. Pierrard, M. Lazar, and S. Štverák, Solar wind plasma properties organized by flow speed, Solar Phys. **295**, 151 (2020).

[15] M. Lazar and H. Fichtner (eds.), *Kappa Distributions* (Springer, Switzerland, 2021).

[16] H. J. Metcalf and P. van der Straten, *Laser Cooling and Trapping* (Springer-Verlag, New York, 1999).

[17] S. Chapman and T. G. Cowling, *The Mathematical Theory of Nonuniform Gases* (Cambridge Mathematical Library, Cambridge, UK, 1991).

[18] S. R. de Groot and P. Mazur, *Nonequilibrium Thermodynamics* (Dover, Mineola, NY, 1984).

[19] T. Schmiel and U. Seifert, Stochastic thermodynamics of chemical reaction networks, J. Chem. Phys. **126**, 044101 (2007).

[20] U. Seifert, Stochastic thermodynamics, fluctuation theorems and molecular machines, Rep. Prog. Phys. **75**, 126001 (2012).

[21] D. Forastiere, R. Rao, and M. Esposito, Linear stochastic thermodynamics, New J. Phys. **24**, 083021 (2022).

[22] L. A. Viehland, *Gaseous Ion Mobility, Diffusion and Reaction* (Springer, Cham, 2018).

[23] R. E. Robson, R. D. White, and M. Hildebrandt, *Fundamentals of Charged Particle and Transport in Gases and Condensed Matter* (CRC Press, Boca Raton, FL, 2018).

[24] A. Santos, *A Concise Course on the Theory of Classical Liquids* (Springer, Cham, 2016).

[25] H. Risken, *The Fokker-Planck Equation, Methods of Solution and Applications*, 2nd ed. (Springer, Berlin, 1996).

[26] K. Andersen and K. E. Shuler, On the relaxation of the hard-sphere Rayleigh and Lorentz gas, J. Chem. Phys. **40**, 633 (1964).

[27] M. H. Alexander, G. E. Hall, and P. J. Dagdigian, The approach to equilibrium, detailed balance and the Master equation, J. Chem. Educ. **88**, 1538 (2011).

[28] P. Viegas, M. C. M. van de Sandem, S. Longo, and P. Diomede, Validation of the Fokker-Planck approach to vibrational kinetics in CO_2 plasma, J. Phys. Chem. C **123**, 22823 (2019).

[29] B. Shizgal and D. R. A. McMahon, Electric field dependence of transient electron transport properties in rare gas moderators, Phys. Rev. A **32**, 3669 (1985).

[30] B. Shizgal and K. Ness, Thermalization and annihilation of positrons in helium, J. Phys. B: At. Mol. Phys. **20**, 847 (1987).

[31] B. Shizgal, The coupling of electron thermalization and electron attachment; SF_6 and CCl_4 in rare gas moderators, J. Phys. B: At. Mol. Opt. Phys. **21**, 1699 (1988).

[32] G. Lebon, D. Jou, and J. Casas-Vazquez, *Understanding Non-Equilibrium Thermodynamics* (Springer, Berlin, 2008).

[33] S. P. Christon, D. G. Mitchell, D. J. Williams, L. A. Frank, C. Y. Huang, and T. E. Eastman, Energy spectra of plasma sheet ions and electron from 50 eV/e to 1 MeV during plasma temperature transitions, J. Geophys. Res. **93**, 2562 (1988).

[34] M. Maksimovic, V. Pierrard, and J. F. Lemaire, Kinetic model of the solar wind with Kappa distribution functions in the corona, Astron. Astrophys. **324**, 725 (1997).

[35] M. Maksimovic, V. Pierrard, and P. Riley, Ulysses electron distributions fitted with Kappa functions, Geophys. Res. Lett. **24**, 1151 (1997).

[36] M. Maksimovic, S. P. Gary, and R. M. Skong, Solar wind electron suprathermal strength and temperature gradients: Ulysses observations, J. Geophys. Res. **105**, 18337 (2000).

[37] G. Livadiotis and D. J. McComas, Understanding Kappa distributions: A toolbox for space science and astrophysics, Space Sci. Rev. **175**, 183 (2013).

[38] G. Livadiotis, *Kappa Distributions* (Elsevier, Amsterdam, 2017).

[39] V. Pierrard and M. Lazar, Kappa distributions: Theory and applications in space plasmas, Solar Phys. **267**, 153 (2010).

[40] G. Livadiotis and D. J. McComas, Beyond Kappa distributions: Exploiting Tsallis statistical mechanics in space plasmas, J. Geophys. Res. **114**, A11105 (2009).

[41] B. D. Shizgal, Kappa and other nonequilibrium distributions from the Fokker-Planck equation and the relationship to Tsallis entropy, Phys. Rev. E **97**, 052144 (2018).

[42] A. Hasegawa, K. Mima, and M. Duong-van, Plasma Distribution Function in a Superthermal Radiation Field, Phys. Rev. Lett. **54**, 2608 (1985).
[43] W. Koepf and M. Masied-Jamei, A generalization of Student's t-distribution from the viewpoint of special functions, Integr. Transf. Spec. F. **17**, 863 (2006).
[44] M. Shakil, B. M. Golam Kibria, and J. Narim Singh, A new family of distributions based on the generalized Pearson differential equation with some applications, Austrian J. Stat. **39**, 259 (2010).
[45] M. Shakil, B. M. G. Kibria, and J. N. Singh, Characterization of a new class of generalized Pearson distribution by truncated moment, Int. J. Comp. Theo. Stat. **3**, 91 (2016).
[46] H. Patel and B. D. Shizgal, Pseudospectral solutions of the Fokker-Planck equation for Pearson diffusion that yields a Kappa distribution; the associated SUSY Schrödinger equation, Comp. Theor. Chem. **1194**, 113059 (2021).
[47] B. D. Shizgal, Energetic particle distributions in space physics represented by the Pearson differential equation for the Kappa distribution: II, Astrophys. Space Sci. **367**, 7 (2022).
[48] B. D. Shizgal, Energetic particle distributions in space physics represented by the Pearson differential equation for the Kappa distribution, Astrophys. Space Sci. **366**, 50 (2021).
[49] A. Dechant, S. T. Shafier, D. A. Kessler, and E. Barkai, Heavy-tailed phase-space distributions beyond Boltzmann-Gibbs: Confied laser-cooled atoms in a nonthermal state, Phys. Rev. E **94**, 022151 (2016).
[50] T. S. Biró and A. Jakovác, Power-Law Tails from Multiplicative Noise, Phys. Rev. Lett. **94**, 132302 (2005).
[51] L. Borland, Ito-Langevin equations within generalized thermostatics, Phys. Lett. A **245**, 67 (1998).
[52] E. Lutz, Anomalous diffusion and Tsallis statistics in an optical lattice, Phys. Rev. A **67**, 051402(R) (2003).
[53] E. Lutz, Power–Law Tail Distributions and Nonergodicity, Phys. Rev. Lett. **93**, 190602 (2004).
[54] T. Wada, A nonlinear drift which leads to κ-generalized distributions, Eur. Phys. J. B **73**, 287 (2010).
[55] T. Wada, A. M. Scarfone, and H. Matsuzoe, On the canonical distributions of a thermal particle in a generalized velocity-dependent potential, Physica A **541**, 123273 (2020).
[56] W. Zhang and B. D. Shizgal, Fokker-Planck equation for Coulomb relaxation and wave-particle diffusion: Spectral solution and the stability of the Kappa distribution to Coulomb collisions, Phys. Rev. E **102**, 062103 (2020).
[57] M. P. Leubner, A nonextensive entropy approach to Kappa-distributions, Astrophys. Space Sci. **282**, 573 (2002).
[58] M. P. Leubner and Z. Vörös, A nonextensive entropy approach to solar wind intermittency, Astrophys. J. **618**, 547 (2005).
[59] B. Shizgal, *Spectral Methods in Chemistry and Physics: Applications to Kinetic Theory and Quantum Mechanics* (Springer, Dordrecht, 2015).
[60] J. S. Chong and G. Cooper, A practical difference scheme for Fokker-Planck equations, J. Comput. Phys. **6**, 1 (1970).
[61] I. S. Gradshteyen and J. M. Ryzik, *Tables of Integrals, Series and Products* (Elsevier, Amsterdam, 2007), Sec. 2.103.5, p. 67.
[62] C. Tsallis, The nonadditive entropy S_q and its application in physics and elsewhere: Some remarks, Entropy **13**, 1765 (2011).
[63] D. A. Stariolo, The Langevin and Fokker-Planck equations in the framework of a generalized statistical mechanics, Phys. Lett. A **185**, 262 (1994).
[64] A. Comtet, A. D. Bandrauk, and D. K. Campell, Exactness of semiclassical bound state energies for supersymmetric quantum mechanics, Phys. Lett. B **150**, 159 (1985).
[65] F. Cooper, A. Khare, and U. Sukhatme, Supersymmetry and quantum mechanics, Phys. Rep. **251**, 267 (1995).
[66] K. Leung, B. D. Shizgal, and H. Chen, The Quadrature Discretization Method (QDM) in comparison with other numerical methods of solution of the Fokker-Planck equation for electron thermalization, J. Math. Chem. **24**, 291 (1998).
[67] P. H. Yoon, Non-equilibrium statistical mechanical approach to the formation of non-Maxwellian electron distribution in space, Eur. Phys. J. Spec. Top. **229**, 819 (2020).
[68] C.-Y. Ma and D. Summers, Formation of power-law energy spectra in space plasmas by stochastic acceleration due to whistler-mode waves, Geophys. Res. Lett. **25**, 4099 (1998).
[69] C. W. Gardiner, *Stochastic Methods*, 4th ed. (Springer, Berlin, 2009).
[70] T. M. Cover and J. A. Thomas, *Elements of Information Theory* (Wiley-Interscience, New York, 2006).
[71] E. Lutz and F. Renzoni, Beyond Boltzmann-Gibbs statistical mechanics in optical lattices, Nat. Phys. **9**, 615 (2013).
[72] B. Shizgal, Electric-field-dependent bimodal distribution functions for electrons in argon, xenon, and krypton owing to the Ramsauer-Townsend minima in the electron-atom momentum-transfer cross sections, Phys. Rev. A **106**, 022805 (2022).
[73] Y. Huang and B. Shizgal, Time evolution of electron distributions to bimodal steady states for electrons dilutely dispersed in the inert gases Ar, Kr, and Xe with deep Ramsauer Townsend minima in the momentum transfer cross section, Phys. Scr. **98**, 055403 (2023)